EARTH SURFACE PROCESSES AND LANDFORMS
Earth Surf. Process. Landforms **40**, 995–1005 (2015)

Published online 5 December 2014 in Wiley Online Library
(wileyonlinelibrary.com) DOI: 10.1002/esp.3676

Process-based modeling of kilometer-scale alongshore sandbar variability

D. J. R. Walstra,[1,2]* B. G. Ruessink,[3] A. J. H. M. Reniers[1,2] and R. Ranasinghe[2,4]
[1] Delft University of Technology, Faculty of Civil Engineering and Geosciences, Hydraulic Engineering Section, PO Box 5048, 2600 GA, Delft, The Netherlands
[2] Deltares, Unit Marine and Coastal Systems, Applied Morphology Department, PO Box 177, 2600 MH, Delft, The Netherlands
[3] Utrecht University, Institute for Marine and Atmospheric Research, Faculty of Geosciences, Department of Physical Geography, PO Box 80115, 3508 TC, Utrecht, The Netherlands
[4] UNESCO-IHE, PO Box 3015, 2601 DA, Delft, The Netherlands

Received 25 January 2014; Revised 3 November 2014; Accepted 12 November 2014

*Correspondence to: D. J. R. Walstra, Deltares, Unit Marine and Coastal Systems, Applied Morphology Department, PO Box 177, 2600 MH, Delft, The Netherlands.
E-mail: dirkjan.walstra@deltares.nl

ESPL
Earth Surface Processes and Landforms

ABSTRACT: Subtidal nearshore sandbars may exhibit cyclic net offshore migration during their multi-annual lifetime along many sandy coasts. Although this type of behavior can extend continuously for several kilometers, alongshore variations in cross-shore bar position and bar amplitude are commonly observed. Alongshore variability is greatest when bars display km-scale disruptions, indicative of a distinct alongshore phase shift in the bar cycle. An outer bar is then attached to an inner bar, forming a phenomenon known as a bar switch. Here, we investigate such large-scale alongshore variability using a process-based numerical profile model and observations at 24 transects along a 6 km section of the barred beach at Noordwijk, The Netherlands. When alongshore variability is limited, the model predicts that the bars migrate offshore at approximately the same rate (i.e. the bars remain in phase). Only under specific bar configurations with high wave-energy levels is an increase in the alongshore variability predicted. This suggests that cross-shore processes may trigger a switch in the case of specific antecedent morphological configurations combined with storm conditions. It is expected that three-dimensional (3D) flow patterns augment the alongshore variability in such instances. In contrast to the observed bar behaviour, predicted bar morphologies on either side of a switch remain in different phases, even though the bars are occasionally located at a similar cross-shore position. In short, the 1D model is not able to remove a bar switch. This data-model mismatch suggests that 3D flow patterns are key to the dissipation of bar switches. Copyright © 2014 John Wiley & Sons, Ltd.

KEYWORDS: alongshore variability; sandbars; bar switching; morphodynamic modeling; process based modeling; cyclic bar behavior; Unibest-TC; Noordwijk; Argus; Jarkus

Introduction

Subtidal sandbars are ubiquitous features in the nearshore zone; their number can range from one (Lippmann and Holman, 1990), mostly on swell-dominated coasts, to three or four on storm-dominated coasts (Van Enckevort and Ruessink, 2003a; Castelle *et al.*, 2007; Ruggiero *et al.*, 2009). In general, the individual bars in a multiple-barred system have a multi-annual lifetime, during which they can behave in a gradual cyclic, offshore directed manner (Ruessink and Kroon, 1994; Plant *et al.*, 1999; Shand *et al.*, 1999; Kuriyama, 2002; Ruessink *et al.*, 2003a; Ruggiero *et al.*, 2009; Aagaard *et al.*, 2010). Bars have also been observed to migrate offshore in a rather abrupt manner in response to extreme storm events (Ruessink *et al.*, 2009) as well as net onshore (Aagaard *et al.*, 2004). Here, we focus on the more typical gradual offshore migration. Offshore cycle periods vary worldwide between approximately 1 and 15 years (Shand *et al.*, 1999). The net offshore bar migration is the result of gradual onshore movement during calm periods combined with episodic strong offshore movement during storms (Van Enckevort and Ruessink, 2003a; Walstra *et al.*, 2012). Bars are generated in the intertidal or uppermost subtidal zone. Storm events typically cause the bars to grow, whereas calm conditions lead to bar decay, especially when waves are shore-normally incident (Ruessink *et al.*, 2007; Pape *et al.*, 2010). However, the net bar amplitude response depends on the cross-shore position (Walstra *et al.*, 2012). As a bar moves offshore towards the middle of the surf zone, it increases in height and width. Bar decay sets in when it approaches the seaward limits of the surf zone. Due to the larger water depth the net offshore migration rate gradually decreases and also causes a reduction in the strength of the breaking wave induced longshore currents. As demonstrated in Walstra *et al.* (2012), this results in cross-shore sediment transport gradients that promote bar decay.

Cyclic bar behavior often shows strong alongshore coherence (Ruessink and Kroon, 1994; Wijnberg and Terwindt, 1995; Shand *et al.*, 1999; Kuriyama, 2002), indicating that this phenomenon is not the result of alongshore propagating shore oblique bars (Ruessink *et al.*, 2003a; Walstra *et al.*, 2012).

This implies that transport gradients induced by cross-shore hydrodynamics are dominant over gradients originating from longshore processes where this cyclic bar behavior is concerned. Using a process-based profile model (i.e. assuming alongshore uniformity), Walstra *et al.* (2012) showed that the transient inter-annual bar amplitude response is primarily governed by the water depth above the bar crest, h_{Xb}, and the incident wave angle, θ.

Although the alongshore coherent net offshore migration dominates bar behavior at inter-annual time scales, bars also display alongshore non-uniformities on temporal scales of days to years and spatial scales of 100 m to 2 km (Shand and Bailey, 1999). Processes governing the initiation and evolution of small-scale alongshore non-uniformities such as rip cells and crescentic plan shapes, O(100 m, days to weeks) are now quite well understood (Ranasinghe *et al.*, 2004; Reniers *et al.*, 2004a; Holman *et al.*, 2006; Garnier *et al.*, 2013). On the other hand, the physics governing larger scale alongshore non-uniformities, such as bar switching, are less well known. Bar switching is typically an indication of a distinct phase shift in the bar cycle (Wijnberg and Wolf, 1994; Wijnberg and Terwindt, 1995; Shand, 2003) where an outer bar is attached to an inner bar (Figure 1(a)) or where bars are detached completely, resulting in a fork-like configuration (Figure 1(b)). Although bars can switch under natural conditions, shoreface nourishments may also trigger switches. For example at Noordwijk, The Netherlands, the net offshore bar migration was delayed immediately landward of a shoreface nourishment, while elsewhere net offshore bar migration continued. This spatially discontinuous offshore migration resulted in bar switches that lasted about one year (Ojeda *et al.*, 2008). Under natural conditions bar switching has a relatively large inter-site variation in the associated temporal scales (months to years; Shand *et al.*, 2001) while the alongshore length of the transition zones can differ at least one order of magnitude (100 s of m versus km). Bar switches initiate at the seaward limit of the surf zone, and once established, show limited cross-shore migration (Shand *et al.*, 2001). However, their alongshore migration can be several kilometers during their lifetime (Ruessink and Kroon, 1994; Wijnberg and Terwindt, 1995).

Although natural and nourishment-induced bar switching events are largely similar, little is known about the physical processes that govern this type of morphological response under natural conditions. Shand *et al.* (2001) found that only shore oblique energetic wave conditions triggered bar switching events. However, as not all high energy events resulted in bar switching, Shand *et al.* (2001) concluded that other factors such as the antecedent morphology could play a controlling role too. Furthermore, Shand *et al.* (2001) suggested that the observed regularity in the alongshore bar switching locations (both at Wanganui and the Dutch coast) could be an indication of regional hydrodynamic controls or a link to alongshore changes in cross-shore slope or the number of bars.

Because cross-shore processes dominate the cyclic bar behavior (Walstra *et al.*, 2012), it is likely that this also applies to the local bar morphology on either side of a bar switch. For example, small variability in water depth along an initially coherent bar could trigger different migration rates that ultimately result in a switch. Therefore, the objective of the present paper is (1) to establish to what extent cross-shore processes can initiate, amplify or dampen alongshore sandbar variability at the km-scale, and (2) to identify the relative importance of wave forcing and antecedent morphology on the predicted large-scale alongshore variability. This study focuses on a double barred beach located along the storm dominated Dutch coast during a time it was unaffected by nourishments.

To reach our aims, we apply a process based cross-shore profile model (Ruessink *et al.*, 2007; Walstra *et al.*, 2012) on 24 transects with an alongshore spacing of 250 m at a 6 km coastal section near Noordwijk in The Netherlands (Figure 2). During the period considered, continuous alongshore bars are followed by natural bar switching events which in time transform back to continuous alongshore bars. In the model the (bar) morphology evolves because of the cross-shore feedback between the hydrodynamics (waves and currents), sediment transport and the morphology itself (Van Rijn *et al.*, 2013). We selected this model for two reasons: (1) to our knowledge process-based area models have not been able to predict accurately inter-annual bar morphology behavior (Grunnet *et al.*, 2004; Van Duin *et al.*, 2004; Ruggiero *et al.*, 2009); and (2) detailed evaluation of the wave forcing would not be possible as acceptable run times require a significant reduction in the number of wave conditions (Walstra *et al.*, 2013).

To identify the importance of cross-shore processes, model predictions initialized with a relatively alongshore uniform set of profiles are compared with predictions starting in a year

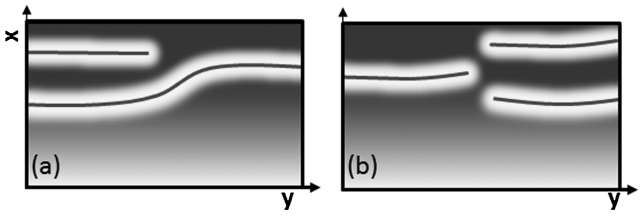

Figure 1. Schematic overview of two bar switch configurations: (a) bar switch where the outer bar is attached to the inner bar of alongshore uniform bars; and (b) fork-like bar switch configuration with a complete alongshore separation of the bars. The colors specify depth in a relative sense; the thin blue lines in the yellow bands indicate the bar crests. This figure is available in colour online at wileyonlinelibrary.com/journal/espl

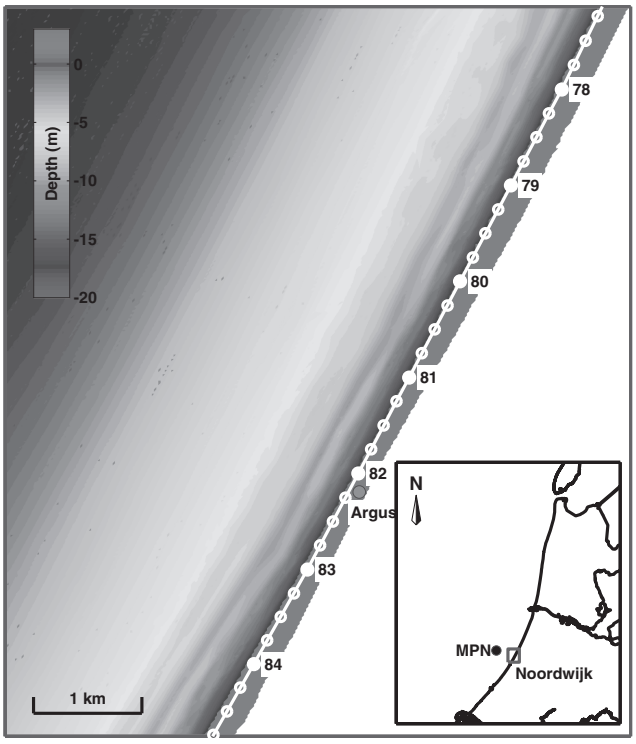

Figure 2. The Noordwijk coast with the beachpoles representing the alongshore coordinate system. The location of the ARGUS video system and the wave station MPN are also indicated. This figure is available in colour online at wileyonlinelibrary.com/journal/espl

when a bar switch was present. Next, the relative importance of the wave forcing and the initial morphology are investigated for nine simulation periods. For each period, hindcast simulations act as a reference for simulations in which either the wave forcing or the initial profiles were modified.

Observations

Study site

Noordwijk is located within the central part of the 120-km-long uninterrupted Dutch coast, faces northwest (298°N) and is more than 20 km away from the most nearby harbor moles (Figure 2). Offshore wave recordings, available from 1979 to 2002 in 18 m water depth (Meetpost Noordwijk – MPN – about 5 km offshore, see Figure 2), indicate an average offshore root-mean-square wave height (H_{rms}) of 0.7 m and a corresponding peak wave period of 6 s. Waves are mainly incident from south-west to north-west. Storm waves are primarily obliquely incident and occur throughout the year, although autumn and winter are usually slightly more energetic (storms with offshore wave heights of about 3–4 m typically occur two to three times in the autumn–winter season). The tide at Noordwijk is semi-diurnal with a 1 m and a 1.8 m range at neap and spring tide, respectively. Storm surges can raise the water level by more than 1 m above the astronomical tide level. Because bar dynamics are, in part, governed by the water depth above the bar, h_{Xb}, measured water levels at IJmuiden are directly imposed as boundary conditions.

Using annual depth surveys with a 250 m longshore resolution spanning nearly three decades, Wijnberg and Terwindt (1995) showed that the site is characterized by a shore-parallel double subtidal bar system that experiences inter-annual net offshore migration with occasional bar switches. The bar cycle, marked by the period between two bar decay events, takes about 3 to 4 years to complete. During storms, the outer bar decays and the inner bar migrates offshore to become the new outer bar. Also an intertidal bar is usually present, but with a substantial shorter lifetime (weeks to one month), which at first glance suggests no correlation with the subtidal bar cycle (Quartel *et al.*, 2007). However, the decay of the outer bar initiates a cascaded response which also causes the intertidal bar to migrate offshore towards the subtidal region and to become the new inner bar, thus perpetuating the cycle (Walstra *et al.*, 2012). The residual inter-annual offshore bar migration at Noordwijk was confirmed by Van Enckevort and Ruessink (2003a, 2003b) based on daily observations of the inner and outer bar crest positions from 1995 to 1998 derived from video imagery between $y = 79$ km and $y = 81.75$ km (distances are defined in a local longshore coordinate system, see also Figure 2). Although on shorter time scales small alongshore non-uniform features such as rip channels were observed, these did not appear to affect the inner and outer bar behavior on inter-annual time scales. Detailed comparisons of the alongshore variability of the bar crest locations based on the annual Jarkus surveys and the daily Argus surveys clearly showed that the annual surveys were sufficient to capture the inter-annual bar morphology (not shown). In the following, we consider a 6 km section at the coast of Noordwijk from $y = 78$ km to $y = 84$ km.

Site-averaged sandbar behavior

Following Plant *et al.* (1999), we summarize the observed development of the 6 km coastal section at Noordwijk in Figure 3(a) with a time stack of the alongshore averaged profile perturbations, $Z'_y(x,t)$, from the start of the surveys in 1965 to 2010:

$$Z'_y(x,t) = \sum_{y=78}^{y=83.75} Z'_t(x,y,t)/N_Y \tag{1}$$

The perturbations $Z'_t(x,y,t)$ were determined by subtracting the time-averaged bathymetry from the surveyed bathymetries, Z, as:

$$Z'_t(x,y,t) = Z(x,y,t) - \sum_{t=1965}^{t=1998} Z(x,y,t)/N_t \tag{2}$$

Here N_Y is the number of cross-shore profile locations, N_t is the number survey dates between 1965 and 1998, x is the (equidistant) cross-shore coordinate, y the longshore coordinate and t denotes time. The surveys from 1999 onwards were not considered in the time-averaged bathymetry as the shoreface at Noordwijk was regularly nourished since that time (Ojeda *et al.*, 2008).

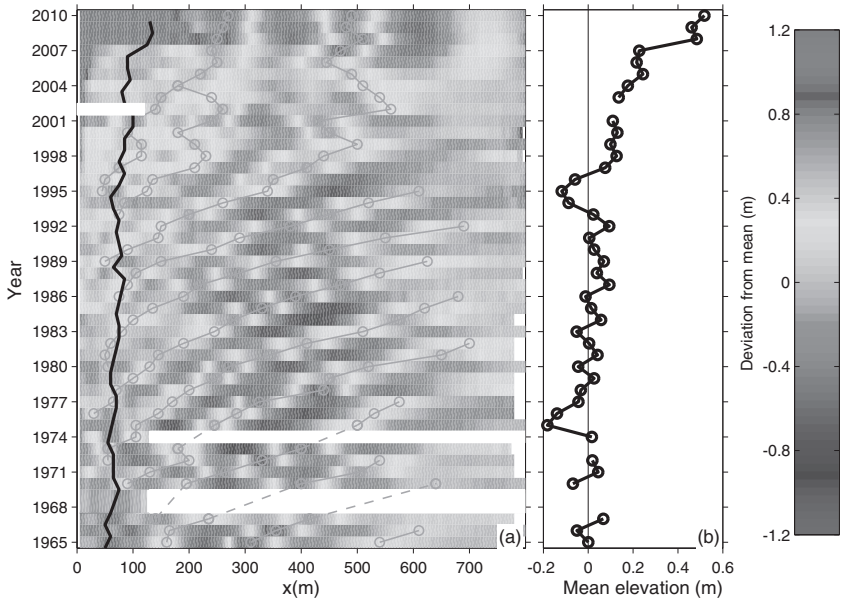

Figure 3. (a) Time stack of alongshore-averaged depth deviations (y = [78:84] km) from the 25-year mean profile. Black line indicates the alongshore averaged shoreline ($z = 0$ m) position ($x = 0$ m is at the 2005 dune foot positions $z = +3$ m), the gray lines indicate alongshore averaged bar crest positions. (b) Time series of cross-shore averaged profile perturbations from Figure 3(a). This figure is available in colour online at wileyonlinelibrary.com/journal/espl

The distinct signature of the alongshore averaged cyclic offshore bar migration visible in Figure 3(a) confirms previous observations (Wijnberg and Terwindt, 1995; Walstra *et al.*, 2012) and highlights that bar migration is alongshore coherent and dominates the long-term morphology throughout the 1965 to 1998 period. Nourishments have a profound impact on the bar morphology from 1999 onwards. Consistent with observations elsewhere along the Dutch coast (Van Duin *et al.*, 2004; Grunnet and Ruessink, 2005), the bars have migrated somewhat shoreward and the net offshore migration has been absent since 1999 (see also Ojeda *et al.*, 2008).

Cross-shore averaging of $Z_y'(x,t)$ allows us to determine the degree to which mass was conserved in the study area (Figure 3(b)). Although a small increasing trend is present, changes in mean elevation are limited and seem to be within, or close to, the ranges of the measurement accuracy (Wijnberg and Terwindt, 1995) until 1998. From 1999 onwards, the nourishments clearly induce an increasing mean elevation. The local mean elevation minima in 1975–1976 and 1994–1996 (Figure 3(b)) are correlated with periods when the outer bar had migrated beyond the seaward limit of the surveys (at approximately 8 m water depth) and the new outer bar had not yet reached its maximum amplitude. The local maxima in mean elevations (e.g. 1979, 1981, 1984, 1987 and 1992) coincided primarily with periods when the middle bar was most pronounced and the outer bar had not yet decayed and/or migrated offshore. Therefore, the inter-annual fluctuations of the mean elevation within the survey area are correlated with the alongshore averaged phase of the bar cycle. The life cycle (i.e. bar initiation near the water line followed by gradual growth and offshore migration and finally the decay at the seaward limit of the surf zone) of 7 bars was fully captured. As can be seen in Figure 3(a), each bar life cycle was approximately 10 years. Overall, prior to the nourishments, the bars had fairly similar amplitude response and migration characteristics. The bar crest, indicated by the gray lines, run more or less parallel in Figure 3(a) and the bars amplitude grow and decay in approximately the same cross-shore regions.

Intra-site variability in sandbar behavior

From here onwards, only the period from 1987 to 1998 is considered in detail as this period encompassed the full life cycle of the two most recent bars unaffected by nourishments (i.e. bars that were present in the years 1986–1995 and 1989–1998, respectively, see also Figure 3). Furthermore, this period encompassed two distinct episodes of bar switching alternating with periods of more alongshore coherent behavior (Figure 4). The first bar switch occurred from 1988 to 1989. Because the outer bar in 1987 was fairly alongshore uniform, this bar switch originated from a distinct alongshore difference in net offshore migration rates or bar amplitude response between 1987 and 1988. The outer bar in the southern section ($y = 82$ km to $y = 84$ km) experienced a relatively large bar amplitude decay compared with the northern section ($y = 78$ km to $y = 82$ km, Figure 4(b)). In 1988 some remains of the outer bar can still be distinguished in the northern section, which suggests that the offshore migration was approximately similar for the entire section. However, when considering the bar crest location, the 1988 morphology resembles the schematic bar switch configuration in Figure 1(a). The outer bar amplitude decay at the southern section enhanced the offshore migration of the inner bar, which by 1989 (Figure 4(c)) resulted in a breakup of the 1988 inner bar that resembles the fork-like bar switch configuration shown schematically in Figure 1(b). One year later a similar kind of response can be observed for the northern section ($y = 78$ km to $y = 81.25$ km, Figure 4(d)): the decay of the outer bar caused a rapid offshore migration of the inner bar in this region. As a consequence it attached to the outer bar in the southern section, which marked the end of the bar switch period.

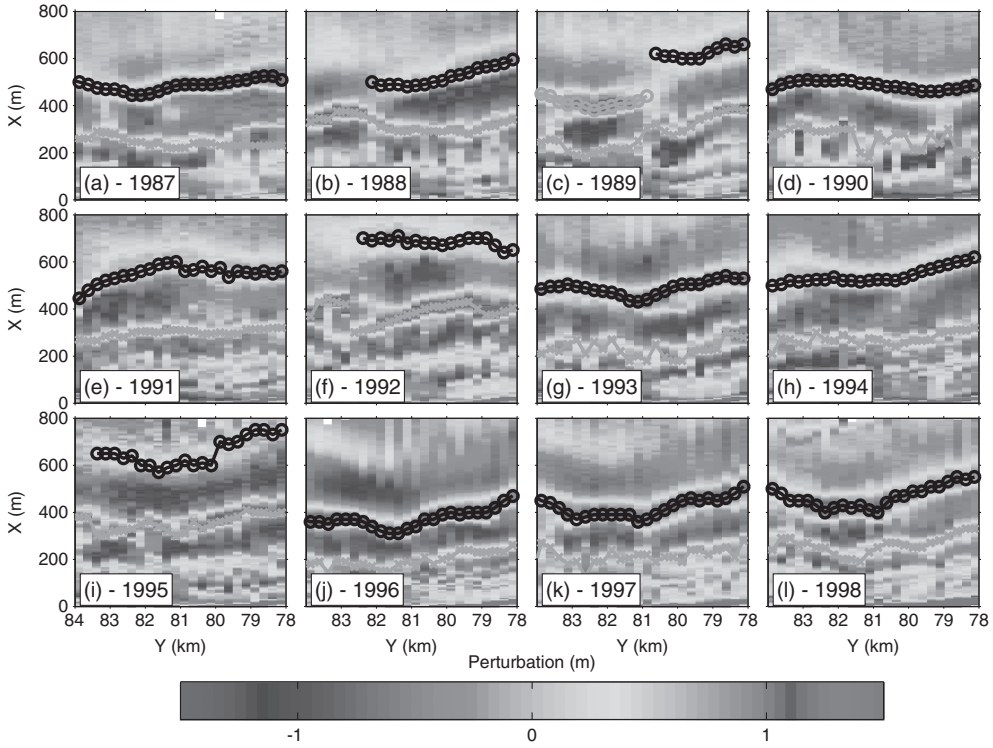

Figure 4. Observed profile perturbations from 1987 to 1998; black circles and grey crosses indicate the outer and inner bar respectively. In 1989 (plot c) the grey circles indicate the alongshore part of the outer bar that was the inner bar in the previous year. This figure is available in colour online at wileyonlinelibrary.com/journal/espl

The 1988–1989 bar switch period resulted in an outer bar with a relatively large alongshore variation in bar amplitude (and h_{Xb}) in 1990 (Figure 4(d)). As a consequence there was a substantial alongshore variation in offshore bar migration from 1990 to 1991. By 1992 this enhanced alongshore outer bar variability caused a similar response to the inner bar causing it to break up at $y = 83$ km (Figure 4(f)). We did not specifically consider this bar switch because it was less pronounced and did not seem to indicate a clear shift in the bar cycle. However, during both bar switching periods, the outer bar response clearly controlled the inner bar development to a large extent.

From 1994 to 1998 the outer bars were relatively alongshore uniform or coherent (Figure 4(h)–(l)). By 1995 a new cycle was initiated as the outer bar by this time had decayed considerably, the new outer bar migrated gradually offshore and was still present in 1998. No bar switching events on intra-annual time scales were observed in the daily video images collected between 1995 and 1998 (Van Enckevort and Ruessink, 2003b).

Model Approach

The first objective (can cross-shore processes initiate, amplify and dampen alongshore sandbar variability on km scale?) was addressed by considering two analysis periods. As the lifespan of the bar switches at Noordwijk were less than the bar cycle period of about 3 years, the analysis interval (and model period) was restricted to this period. The first period comprised the 1987 to 1990 period which is characterized by an initially alongshore uniform morphology from which in the two following years a distinct bar switch evolved, but by 1990 the bar switch had decayed resulting in a relatively alongshore uniform morphology again (see also Figure 4). The second period started in 1989 when the bar switch was most pronounced, followed by 2 years when the bars were alongshore continuous, but in the last year (1992) a bar switch was present again in the middle bar. The first period was used to investigate whether the model was able to develop a bar switch from relatively alongshore uniform profiles. The second period is primarily used to test the ability of the model to dampen a bar switch.

The second objective (establish the relative importance of the wave forcing and the antecedent morphology on the predicted alongshore variability) was addressed by considering nine periods of 3-year hindcast predictions that started with the annually surveyed profiles between 1987 and 1995. These acted as a reference for sets of 3-year simulations in which either the wave forcing or the initial profiles were modified.

Model description

Unibest-TC is a cross-shore profile model and comprises coupled, wave-averaged equations of hydrodynamics (waves and mean currents), sediment transport, and bed level evolution. Straight, parallel depth contours are assumed. Starting with an initial, measured cross-shore depth profile and boundary conditions offshore, the cross-shore distribution of the hydrodynamics and sediment transport are computed. Transport divergence yields bathymetric changes, which feed back to the hydrodynamic model at the subsequent time step, forming a coupled model for bed level evolution. The phase-averaged wave model is based on Battjes and Janssen (1978) extended with the roller model according to Nairn *et al*. (1990) and the breaker delay concept (Roelvink *et al*., 1995) to have an accurate cross-shore distribution of the wave forcing. The cross-shore varying wave height to depth ratio, γ, of Ruessink *et al*. (2003b) was used in the breaking wave dissipation formulation as it results in more accurate estimates of the wave height across bar–trough systems than a cross-shore constant γ. The vertical distribution of the flow velocities is determined with the Reniers *et al*. (2004b) 1DV current model. Based on the local wave forcing, mass flux, tide and wind forcing a vertical distribution of the longshore and cross-shore wave-averaged horizontal velocities are calculated. These advective currents are combined with the instantaneous oscillatory wave motion in such a way that the resulting velocity signal has the same characteristics of short-wave velocity skewness, amplitude modulation, bound infragravity waves, and mean flow as a natural random wave field (Roelvink and Stive, 1989). The transport formulations distinguish between bed load and suspended load transport. The bed load formulations (Ribberink, 1998) are driven by the instantaneous velocity signal. The suspended transports are based on an integration over the water column of the sediment flux. The wave-averaged near-bed sediment concentration is prescribed according to Van Rijn (1993), which among other factors, is driven by a time-averaged bed shear stress based on the instantaneous velocity signal. A detailed description of the Unibest-TC model can be found in Ruessink *et al*. (2007).

The model was forced with wave data measured in about 18 m depth, 5 km offshore. The initial profiles were taken from the Jarkus database (Wijnberg and Terwindt, 1995) and interpolated onto the computational grid with a resolution of 200 m offshore, gradually decreasing to 2 m across the active part of the profile (above 10 m water depth) without any alongshore averaging.

Model simulations

The objectives are addressed through a combined analysis of the observed and the predicted barred cross-shore profile development at the surveyed transects within the 6 km study area. The exact period was defined by the survey dates of the Jarkus profiles 3 years apart. The measured wave and water level data corresponding to the simulation periods were directly imposed on the seaward model boundary. Given the alongshore uniform offshore bathymetry (Figure 2), we assumed no alongshore variation in the wave conditions. This allowed us to force the models at the considered transects with identical wave forcing time series. These reference simulations were carried out for all (24) survey transects within the 6 km study area.

The effect of modified initial profiles and wave forcing was investigated for three periods in which again all 24 survey transects were included:

A. 1987–1990: besides the presence of the bar switch, it was also selected because it was the most energetic period (Figure 5);
B. 1989–1992: because of the bar switch that was present in the 1989 morphology;
C. 1995–1998: during this period no bar switch was present and it had the least energetic wave forcing (Figure 5).

For each of these periods we performed simulations in which either (1) the starting profiles were kept at 1987 or 1989, but forced with the time series of all the considered periods of the reference simulations, or (2) the wave forcing time series was kept at the 1987–1990, 1989–1991 or 1995–1998 periods, but the profiles from 1987 to 1995 were used to initialize the model (see Table I for an overview).

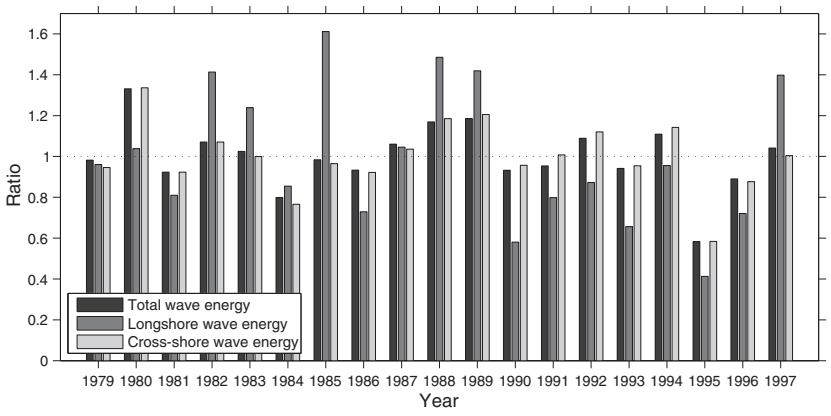

Figure 5. Ratios of the annual mean total, longshore and cross-shore wave energy scaled with the 19 year means (1979–1998). Annual means are based on the period between consecutive annual survey dates.

Table I. Overview of the model simulation scenarios

Scenario	Profile initialization year[a]	Wave forcing start year[b]	Number of simulations[c]
Reference	1987, 1988, 1989, 1990, 1991, 1992, 1993, 1994, 1995	1987, 1988, 1989, 1990, 1991, 1992, 1993, 1994, 1995	216
WF1987[d]	1988, 1989, 1990, 1991, 1992, 1993, 1994, 1995	1987	192
DP1987[e]	1987	1988, 1989, 1990, 1991, 1992, 1993, 1994, 1995	192
WF1989[d]	1987, 1988, 1990, 1991, 1992, 1993, 1994, 1995	1989	192
DP1989[e]	1989	1987, 1988, 1990, 1991, 1992, 1993, 1994, 1995	192
WF1995[d]	1987, 1988, 1989, 1990, 1991, 1992, 1993, 1994	1995	192

[a]All simulations cover the 3-year period between the corresponding survey dates (e.g. 1987 profile initialization represents the simulation from 3-10-1987 to 6-5-1990).
[b]For scenarios indicated by WF, the length of the simulations is determined by the period of wave forcing time series (e.g. WF1995 was initialized with the 1987 to 1994 profiles, but were always run from 3-7-1995 to 10-8-1998).
[c]All 24 ($\Delta y = 250$ m) survey transects between $y = 78$ and 83.75 km were considered.
[d]WF stands for simulations in which a single wave forcing time series was combined with all the considered profiles.
[e]DP stands for simulations in which the profiles of a specific year were combined with all considered wave forcing time series.

The resulting 1176 3-year simulations (Table I) are analyzed in a later section by inter-comparing the morphological development and indicators, introduced in the following section, that describe alongshore variability. First, the reference simulations covering the 1987–1990 and 1989–1992 periods are evaluated; next, the relative influence of the profile initializations and the wave forcing is investigated by comparing the predicted inter-annual bar morphology for the profile and wave forcing scenarios listed in Table I.

Prior to the steps outlined above we first validated the model for the 1995 to 1998 period (during which bars were alongshore continuous) for which all 24 transects were considered. The model's free parameters were set to the values determined in Walstra *et al*. (2012) based on a calibration on the 1984–1987 data for a single transect ($y = 80$ km) at Noordwijk. The 1995–1998 simulation at the same transect yielded a slightly better performance than was achieved by the original calibration, also classifying the validation result for this transect as 'reasonable' according to Van Rijn *et al*. (2003). Furthermore, application of the model on all transects for the 1995–1998 period resulted in 'reasonable' to 'good' agreement according to the Van Rijn *et al*. (2003) classification with, on average, the highest skill in the northern section of the study area.

Indicators of alongshore variability

To evaluate the temporal evolution of the alongshore variability, the alongshore averaged values of the bar crest location, $\langle X_b \rangle$ and the water depth above the bar crest, $\langle h_{Xb} \rangle$ were considered. In the case of discontinuous alongshore bars, these indicators may become unreliable or do not fully capture the morphological variability. Therefore, we also utilized the alongshore variability ratio, $\langle F_{3D} \rangle$, which is based on the variance of the profile perturbations (Plant *et al*., 1999):

$$\langle F_{3D} \rangle = 1 - \frac{1}{N_x} \sum_{x=x_1}^{x=x_{Nx}} [F_{2D}(x)] \tag{3}$$

in which N_x is the number of cross-shore grid points (assuming an equidistant cross-shore distance x). $\langle F_{3D} \rangle$ is the ratio between alongshore non-uniform and total bathymetric variability. A value of 1 implies a fully 3D bathymetry without any alongshore coherence, whereas a value of 0 represent an alongshore uniform bathymetry. In Equation (3) $F_{2D}(x)$ is the cross-shore distribution of the alongshore variability ratio:

$$F_{2D}(x) = \left[\frac{s_{y,t}(x)}{S_{y,t}(x)} \right]^2 \tag{4}$$

in which $s^2_{y,t}(x)$ is the temporal variance of alongshore uniform component

$$s^2_{y,t}(x) = \frac{1}{3}\sum_{t=T_i}^{t=T_{i+3}} \left[Z'_y(x,t)\right]^2 \quad (5)$$

and $S^2_{y,t}(x)$ is the variance of the profile perturbation averaged in both time and alongshore

$$S^2_{y,t}(x) = \frac{1}{3N_y}\sum_{y=78}^{y=83.75}\sum_{t=T_i}^{t=T_{i+3}} \left[Z'_t(x,y,t)\right]^2 \quad (6)$$

T_{i+3} reflects the 3-year duration of the simulations.

Results

Initiation and decay of bar switches (1987–1990 vs. 1989–1992)

We discuss two periods (1987–1990 and 1989–1992) during which a bar switch was initiated (1988) that had vanished 2 years later. First, the simulations starting in 1987 (and ending in 1990) are discussed. Since the bar switch is not present in the 1987 bar morphology, we can investigate whether the cross-shore processes can initiate a bar switch from relatively alongshore uniform bars. The opposite (i.e. can the model predict the end of a bar switch when it is present in the initial bar morphology) is tested with the simulations starting in 1989. The basis of the analysis is a comparison of the observed and predicted profile perturbations. Although the simulations at each transect were independent, we combined the predicted profile development into a top view of the perturbations of the 6 km study area.

The initial (1987) and predicted morphological development from 1988 to 1990 are compared with the observations in Figure 6. The offshore migration and amplitude growth of the inner bar coincided reasonably well after 1 year (year 1988, compare Figure 6(b) and (e)). However, the offshore migration of the outer bar was significantly over-estimated. Besides the over-estimated offshore migration of both bars in the following years, X_b (and also h_{Xb}) remained alongshore coherent, in contrast to the observations. In the southern section the outer bar is interpreted as being no longer present as it has decayed considerably, resulting in a relict feature without alongshore coherence. From 1989 to 1990, the former inner bar (which by now had become the outer bar) was predicted to gradually migrate further offshore. The predicted alongshore variability remained approximately constant. As the bar switch had disappeared by 1990 (Figure6(d)), the final prediction (Figure 6(g)) resembled the observations (Figure 6(d)) fairly well. However, the model completely failed to predict the observed initiation and decay of the bar switch.

Interestingly, similar to the observations, the initial 1989 inner bar switch was almost removed in the predictions (compare Figure 7(b) and (e)). The transformation of the concave shape of the inner bar at $y = 81$ to 84 km in 1989 to a convex shape in 1990 qualitatively agrees with the observations. In the model this change in planshape was caused by the alongshore variability in the water depth above the 1989 bar crest, $h_{x,b}$. At the center of the convex shape ($y = 82.25$ km) the bar was most pronounced (i.e. small $h_{x,b}$) whereas at the distal ends $h_{x,b}$ was initially larger and therefore limited the offshore migration from 1989 to 1990. The alongshore variability of the inner bar was, however, significantly over-estimated. The alongshore variability was predicted to increase with time as the southern section of the bar migrated further offshore and decayed more than the northern section. The enhanced offshore migration in the southern section created accommodation space for a new inner bar, which in 1991 nearly attached to the outer bar at $y = 80.5$ km (Figure 7(f)). However, probably due to the absence of alongshore interaction, this connection did not occur during the following year. By 1992 a new bar switch was present in the observations which showed some similarities with the final predicted morphology.

A common finding from both simulation periods is that the model largely maintains the initial alongshore variability throughout the simulations. As a consequence the model fails to predict the observed generation and decay of bar switches. This is investigated further in the following section.

Relative importance of the wave forcing and the antecedent morphology

The predicted alongshore variability for the 1989–1992 period (Figure 7) was significantly larger than for the 1987–1990 period (Figure 6). Apparently, specific wave forcing combined with the alongshore fluctuations in h_{Xb} present in the initial profiles, amplified the alongshore variability of the bar migration response for the 1989–1992 period, whereas for the 1987–1990 period such a non-linear response appeared to be largely absent. Given the observed variability in both the wave climate (Figure 5) and the observed morphology (Figure 4), we

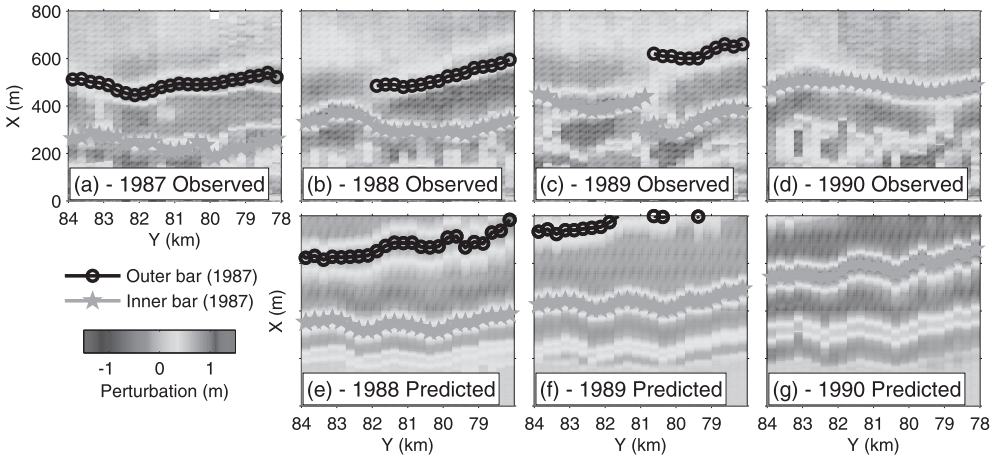

Figure 6. Observed (top row) and predicted (bottom row) profile perturbations from 1987 to 1990, black (grey) line tracks the outer (inner) bar starting from 1987. This figure is available in colour online at wileyonlinelibrary.com/journal/espl

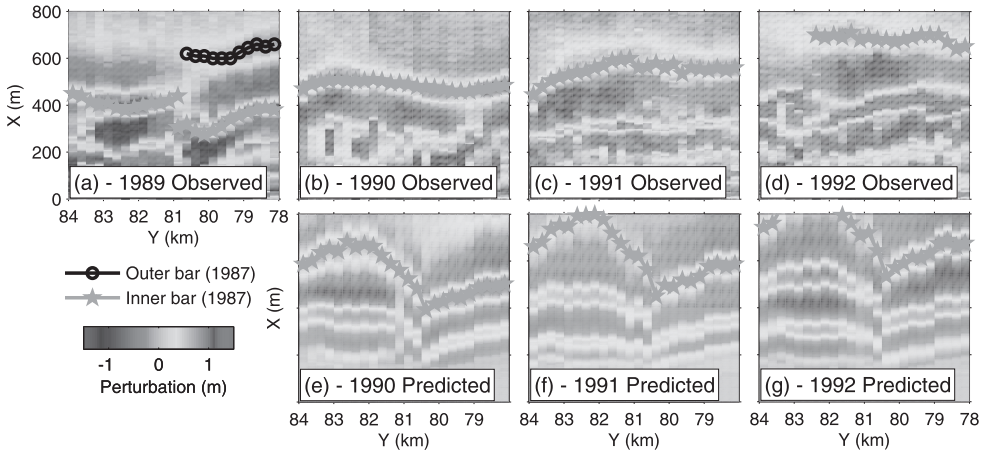

Figure 7. Observed (top row) and predicted (bottom row) profile perturbations from 1989 to 1992, black (grey) line tracks the outer (inner) bar starting from 1987. This figure is available in colour online at wileyonlinelibrary.com/journal/espl

investigate their relative influence on the predicted alongshore variability in this section.

We first analyze the alongshore variability $\langle F_{3D} \rangle$ for the reference cases and all the profile and wave forcing scenarios outlined earlier. Next, the relative importance of the profile initialization and wave forcing is further investigated by considering the bar morphology in greater detail for a number of specific scenarios.

Comparison with the observed $\langle F_{3D} \rangle$ clearly shows that the reference simulations initialized with profiles that contained bar switches (years of initialization: 1988, 1989 and 1992) persistently over-estimated the alongshore variability (compare black and red lines in Figure 8(a)). In contrast, periods that were initially relative alongshore uniform, but during which a bar switch developed within the 3-year simulation period, under-estimated $\langle F_{3D} \rangle$ (e.g. years of initialization: 1987 and 1991). For periods where the observed alongshore uniformity was approximately constant, there was mostly good agreement in $\langle F_{3D} \rangle$ (e.g. years of initialization: 1990, 1993 and 1994).

The $\langle F_{3D} \rangle$ values resulting from the DP1987 and DP1989 scenarios (i.e. respectively initialized with the 1987 or the 1989 profiles) were approximately constant with time (blue and green lines in Figure 8(a)) and similar to their respective 1987 and 1989 reference simulations. In contrast, $\langle F_{3D} \rangle$ resulting from the WF-scenarios showed more agreement with the reference simulations (Figure 8(b)). From this we infer that the initial alongshore variability was the primary source of changes in the predicted $\langle F_{3D} \rangle$ whereas the natural temporal fluctuations in wave energy (Figure 8(c)) were of secondary importance.

These findings are investigated further by considering the bar morphology in more detail for a selected number of simulations. To this end, we compare the temporal evolution of the alongshore averaged values of X_b and h_{Xb} ($\langle \Delta X_b \rangle$ and $\langle \Delta h_{Xb} \rangle$) for four simulations of the WF1989 and WF1995 scenarios: the 1989 and 1995 starting profiles both forced with the 1989–1992 and 1995–1998 wave time series. The predicted $\langle \Delta X_b \rangle$ and $\langle \Delta h_{Xb} \rangle$ evolved very similarly for identical wave forcing during the first 200 days of the simulations (Figure 9(a), (b)). However,

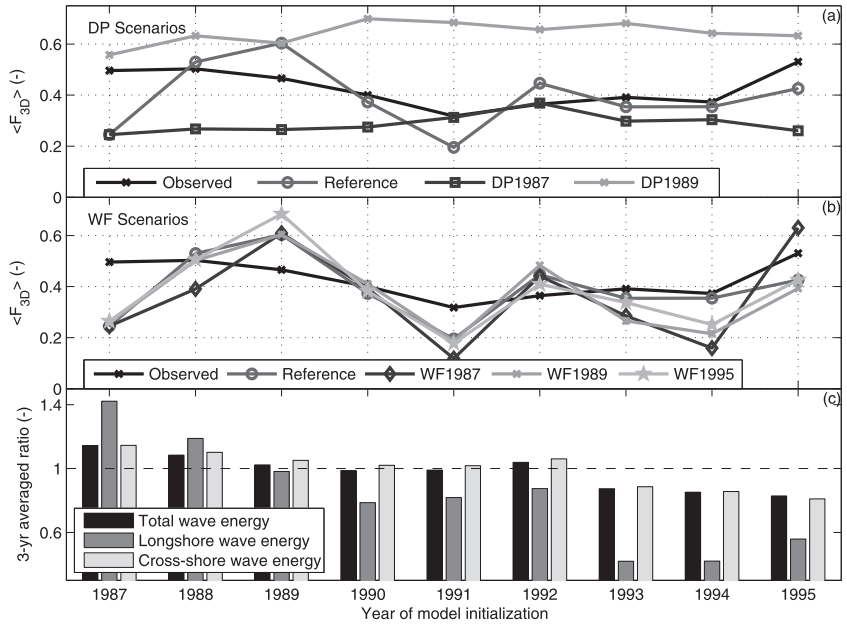

Figure 8. (a) Comparison of the alongshore non-uniform variance with observations (black), reference predictions (red), the DP1987 scenario (blue) and the DP1989 scenario (green, see also Table I for overview of scenarios). (b) Comparison of the alongshore non-uniform variance with observations (black), reference predictions (red), the WF1987 scenario (blue), WF1989 scenario (green) and the WF1995 scenario (cyan). (c) The 3-year averaged wave energy ratios relative to the overall average. This figure is available in colour online at wileyonlinelibrary.com/journal/espl

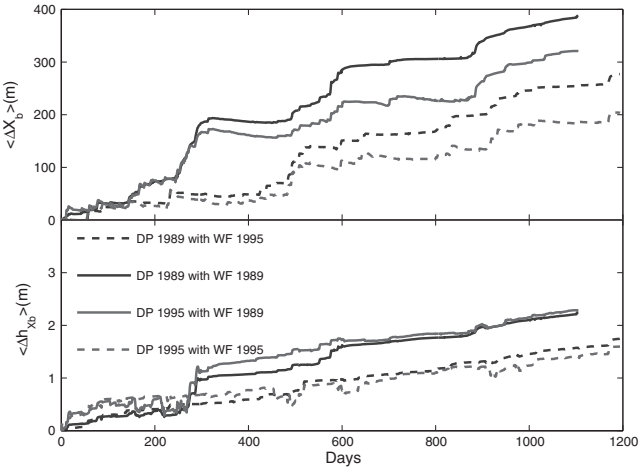

Figure 9. Temporal development relative to the initial value of the longshore averaged ($y = 78$-84 km) (a) outer bar crest positions and (b) the water depth above the bar crest for the reference simulations and simulations initialized with the 1989 and 1995 profiles and imposed with their respective wave forcing time series (WF-scenario, see Table I). This figure is available in colour online at wileyonlinelibrary.com/journal/espl

$\langle \Delta X_b \rangle$ gradually diverged after about 300 days, and even more so after 500 days. The temporal evolution of $\langle \Delta h_{Xb} \rangle$ remained very similar throughout the simulations with identical wave forcing. As the influence of the modified forcing on the bar amplitude development (not shown) was relatively small compared with the changes in h_{Xb}, the morphological response appears to be dominated by the bars migrating towards a common h_{Xb}. As a consequence, the gradually diverging $\langle \Delta X_b \rangle$ (Figure 9(a)) originated from differences in the lower regions of the 1989 and 1995 bed profiles. The more energetic 1989–1991 wave forcing time series result in a further seaward migration and increased $\langle \Delta h_{Xb} \rangle$. Consistent with Ruggiero *et al.* (2009) and Walstra *et al.* (2012), this underlines the importance of h_{Xb} in the bar response.

Despite the clear effect of wave forcing on the alongshore averaged bar morphology, the alongshore variability of the bar crest positions appeared to be relatively unaffected for alongshore uniform initial profiles (Figure 10(a)–(c)). If a bar switch is present in the initial profiles, the alongshore variability was comparable for the bar sections on either side of the bar switch (e.g. north and south of $y = 81.50$ km Figure 10(d)–(f)). However, the alongshore averaged bar morphology at each side of the bar switch responded differently to the modified wave forcing. This is further investigated in Figure 11, where the offshore bar migration at both sides of the bar switch had a dissimilar response to the modified wave forcing. The southern area experienced an accelerated offshore migration relative to the northern area in the case of the more energetic wave forcing (WF1987 and WF1989), whereas such a response was absent for the less energetic wave forcing (WF1995).

Discussion

Because our model is reasonably accurate in the absence of bar switches, we infer that the increased model-error in the presence of bar switches (Figures 6 and 7) is primarily caused by three-dimensional processes, such as flow patterns induced by the alongshore variable morphology which are not accounted for by the model. It is fair to say, however, cross-shore processes also influenced the alongshore variability even to the extent that bar switches were nearly removed when bars at either side of the switch were temporary in a similar phase (Figure 10(d)–(f)). The water depth above the bar crest, h_{Xb}, was found to be of primary importance as, for a given wave forcing, it largely controlled the bar amplitude and bar migration response. For example, the alongshore variations in h_{Xb} in the 1989 profiles resulted in a non-linear morphological response that considerably increased the alongshore variability of the southern section ($y > 81$ km, see Figure 7).

The increased phase differences at either side of the bar switch in the 1988 bathymetry predicted by the WF1987 and WF1989 scenarios were both induced during periods with increased wave action (Figure 11). However, during later periods with similar wave forcing such a response was absent. These outcomes show that a specific state of the morphology subjected to a period with energetic wave forcing can result in an alongshore varying response also when only cross-shore processes are considered. Furthermore, taking into consideration that 3D effects (such as rip currents) could further enhance the alongshore variability, we suspect that the generation of bar switches, similar to the findings of Shand *et al.* (2001), is the outcome of a particular morphological state and wave forcing combination.

Interestingly, the bar growth in the surf zone and bar decay further offshore deviated for identical wave forcing but different initial profiles. This was especially clear for the WF1995 scenario as the alongshore averaged temporal evolution of

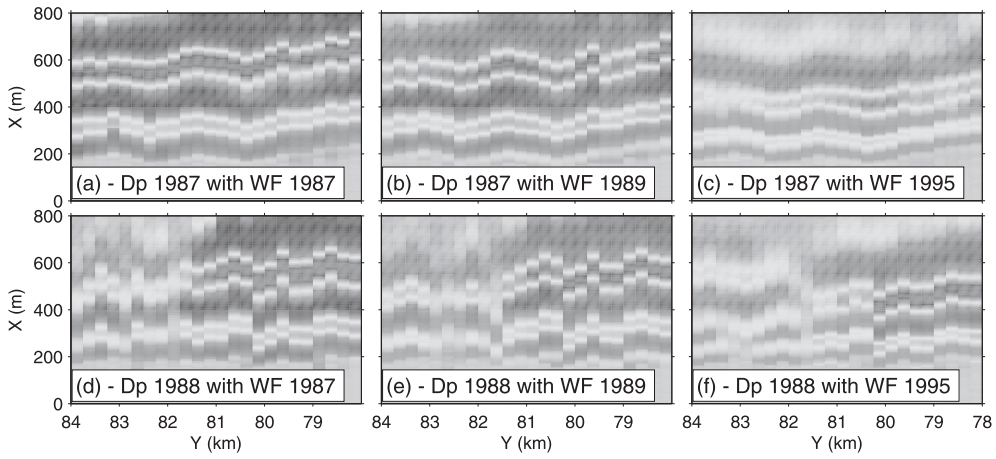

Figure 10. Perturbations of the final predicted morphological development for different combinations of profile initialization and wave forcing time series. Starting from the 1987 (top row) and 1988 (bottom row) profiles imposed with 1987–1990 (left column), 1989–1992 (middle column) and 1995–1998 (right column) wave time series. This figure is available in colour online at wileyonlinelibrary.com/journal/espl

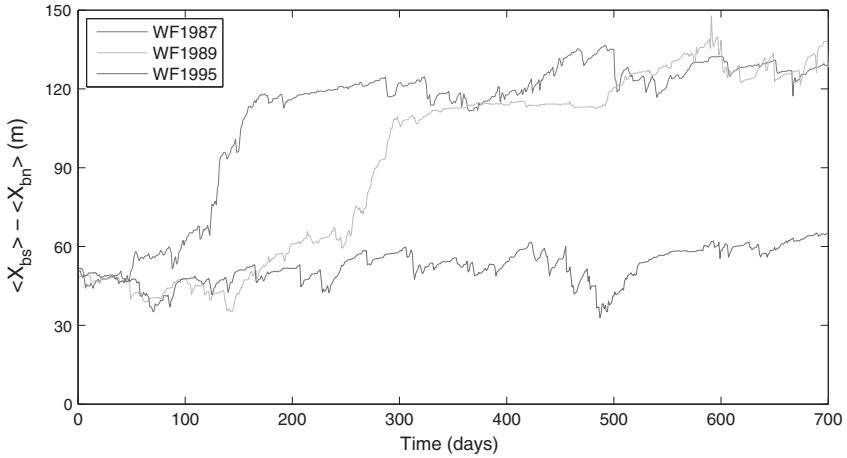

Figure 11. Temporal development of the difference between the alongshore averaged bar position south, $<X_{bs}>$, and north, $<X_{bn}>$, of the bar switch at $y = 81.50$ km for the 1987–1991, 1989–1992 and 1995–1998 wave forcing time series starting from the 1988 profiles. This figure is available in colour online at wileyonlinelibrary.com/journal/espl

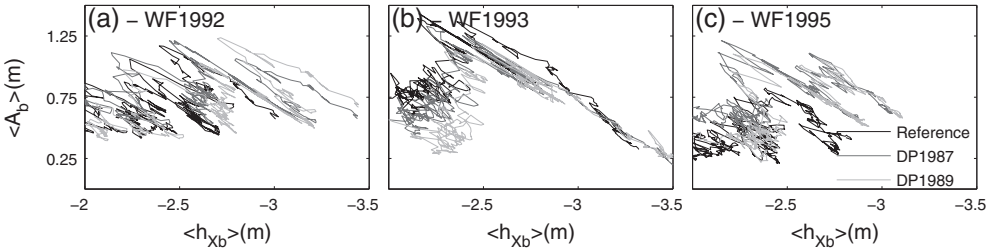

Figure 12. Alongshore averaged bar amplitude, A_b, as a function of the alongshore averaged water depth above the bar crest, h_{Xb}, for various combinations of wave forcing and initial profiles. This figure is available in colour online at wileyonlinelibrary.com/journal/espl

the outer bar amplitude (A_b) as a function of h_{Xb} clearly depended on the initial profiles (Figure 12(c)). For the reference situation (i.e. initialization of the model with the 1995 profiles) the width of the barred profile was significantly smaller as the bar decayed at smaller h_{Xb}, whereas the 1987 and 1989 profile initialisations resulted in a very similar behaviour. Also the maximum bar amplitude was about 0.5 m less for the reference case. For other wave forcing time series the differences were less pronounced, but also in these cases the bar morphology was affected for the entire simulation duration (Figure 12(a), (b)). From these results it is very clear that the initial profiles in combination with specific wave forcing can result in significantly different bar migration characteristics throughout the 3-year simulation period. It is these differences in bar migration that enhance or decrease the migration characteristics at each side of a bar switch and consequently amplify or dissipate the bar switch feature.

Conclusions

When alongshore variability is limited, the model predicts offshore migration of the bars at approximately the same rate (i.e. the bars remain in phase). Only under specific bar configurations and high wave-energy levels is an increase in alongshore variability predicted. This suggests that cross-shore processes may trigger a switch in the case of specific antecedent morphological configurations combined with storm conditions. However, the model is not able to predict the dissipation of a bar switch, as in contrast to the observed bar behavior, predicted bar morphologies on either side of the switch remain in a different phase. The alongshore variability is only temporarily reduced when the bars on either side are occasionally located in a similar cross-shore position. The data–model mismatch suggests that 3D processes play a key role in the generation and decay of bar switches. Potentially 3D flow patterns are responsible for: (1) removing a switch by merging the bars when they were at a similar cross-shore position; or (2) generating a switch after the alongshore variability was amplified under a specific combination of the bar morphology and energetic wave forcing.

Acknowledgements—DJW and RR were supported by Deltares' Coastal Developments (CD) and Coastal Systems (CERM) strategic research programs. RR was also supported by the AXA Research Fund. BGR was funded by the Netherlands Organisation for Scientific Research (NWO) under contract 821.01.012. AR was supported by the National Science Foundation under contract NSF095225.

References

Aagaard T, Davidson-Arnott R, Greenwood B, Nielsen J. 2004. Sediment supply from shoreface to dunes: linking sediment transport measurements and long-term morphological evolution. *Geomorphology* **60**: 205–224. doi: 10.1016/j.geomorph.2003.08.002.

Aagaard T, Kroon A, Greenwood B, Hughes MG. 2010. Observations of offshore bar decay: sediment budgets and the role of lower shoreface processes. *Continental Shelf Research* **30**: 1497–1510. doi: 10.1016/j.csr.2010.05.010.

Battjes JA, Janssen JPFM. 1978. Energy loss and set-up due to breaking of random waves. *Proceedings of the 16th International Conference on Coastal Engineering*. ASCE: New York; 570–587.

Castelle B, Bonneton P, Dupuis H, Sénéchal N. 2007. Double bar beach dynamics on the high-energy meso-macrotidal French Aquitanian Coast: a review. *Marine Geology* **245**: 141–159. doi: 10.1016/j.margeo.2007.06.001.

Garnier R, Falqués A, Calvete D, Thiébot J, Ribas F. 2013. A mechanism for sandbar straightening by oblique wave incidence. *Geophysical Research Letters* **40**: 2726–2730. doi: 10.1002/grl.50464.

Grunnet NM, Ruessink BG. 2005. Morphodynamic response of nearshore bars to a shoreface nourishment. *Coastal Engineering* **52** (7): 119–137. doi: 10.1016/j.coastaleng.2004.09.006.

Grunnet NM, Walstra DJR, Ruessink BG. 2004. Process-based modelling of a shoreface nourishment. *Coastal Engineering* **51**(7): 581–607. doi: 10.1016/j.coastaleng.2004.07.016.

Holman RA, Symonds G, Thornton EB, Ranasinghe R. 2006. Rip spacing and persistence on an embayed beach. *Journal of Geophysical Research* **111**: C01006. doi: 10.1029/2005JC002965.

Kuriyama Y. 2002. Medium-term bar behavior and associated sediment transport at Hasaki, Japan. *Journal of Geophysical Research* **107**(C9): 3132. doi: 10.1029/2001JC000899.

Lippmann TC, Holman RA. 1990. The spatial and temporal variability of sandbar morphology. *Journal of Geophysical Research* **95**: 11575–11590.

Nairn RB, Roelvink JA, Southgate HN. 1990. Transition zone width and implications for modelling surfzone hydrodynamics. *Proceedings of the. 22nd International Conference on Coastal Engineering*. ASCE, 68–91.

Ojeda E, Ruessink BG, Guillen J. 2008. Morphodynamic response of a two-barred beach to a shoreface nourishment. *Coastal Engineering* **55**(12): 1185–1196. doi: 10.1016/j.coastaleng.2008.05.006.

Pape L, Kuriyama Y, Ruessink BG. 2010. Models and scales for nearshore sandbar behavior. *Journal of Geophysical Research, Earth Surface* **115**(F03043): 1–13.

Plant NG, Holman RA, Freilich MH, Birkemeier WA. 1999. A simple model for inter-annual sandbar behavior. *Journal of Geophysical Research – Oceans* **104-C7**: 15 755–15 776.

Quartel S, Ruessink BG, Kroon A. 2007. Daily to seasonal cross-shore behaviour of quasi-persistent intertidal beach morphology. *Earth Surface Processes and Landforms* **32**: 1293–1307. doi: 10.1002/esp.1477.

Ranasinghe R, Symonds G, Black K, Holman R. 2004. Morphodynamics of intermediate beaches: a video imaging and numerical modelling study. *Coastal Engineering* **51**(7): 629–655. doi: 10.1016/j.coastaleng.2004.07.018.

Reniers AJHM, Roelvink JA, Thornton EB. 2004a. Morphodynamic modeling of an embayed beach under wave group forcing. *Journal of Geophysical Research* **109**: C01030. doi: 10.1029/2002JC001586.

Reniers AJHM, Thornton EB, Stanton TP, Roelvink JA. 2004b. Vertical flow structure during sandy duck: observations and modeling. *Coastal Engineering* **51**(3): 237–260. doi: 10.1016/j.coastaleng.2004.02.001.

Ribberink J. 1998. Bed-load transport for steady flows and unsteady oscillatory flows. *Coastal Engineering* **34**(1–2): 52–82. doi: 10.1016/S0378-3839(98)00013-1.

Roelvink JA, Stive MJF. 1989. Bar-generating cross-shore flow mechanisms on a beach. *Journal of Geophysical Research* **94**(C4): 4785–4800.

Roelvink JA, Meijer TJGP, Houwman K, Bakker R, Spanhoff R. 1995. Field validation and application of a coastal profile model. *Proceedings of the Coastal Dynamics 95 Conference*, Gdansk, Poland.

Ruessink BG, Kroon A. 1994. The behaviour of a multiple bar system in the nearshore zone of Terschelling: 1965–1993. *Marine Geology* **121**: 187–197. doi: 10.1016/0025-3227(94)90030-2.

Ruessink BG, Kuriyama Y, Reniers AJHM, Roelvink JA, Walstra DJR. 2007. Modeling cross-shore sandbar behavior on the timescale of weeks. *Journal of Geophysical Research - Earth Surface* **112**(F3): 1–15. doi: 10.1029/2006JF000730.

Ruessink BG, Pape L, Turner IL. 2009. Daily to inter-annual cross-shore sandbar migration: observations from a multiple sandbar system. *Continental Shelf Research* **29**: 1663–1677. doi: 10.1016/j.csr.2009.05.011.

Ruessink BG, Wijnberg KM, Holman RA, Kuriyama Y, van Enckevort IMJ. 2003a. Intersite comparison of interannual nearshore bar behavior. *Journal of Geophysical Research* **108**(C8): 3249. doi: 10.1029/2002JC001505.

Ruessink BG, Walstra DJR, Southgate HN. 2003b. Calibration and verification of a parametric wave model on barred beaches. *Coastal Engineering* **48**(3): 139–149. doi: 10.1016/S0378-3839(03)00023-1.

Ruggiero P, Walstra DJR, Gelfenbaum G, van Ormondt M. 2009. Seasonal-scale nearshore morphological evolution: field observations and numerical modeling. *Coastal Engineering* **56**: 1153–1172. doi: 10.1016/j.coastaleng.2009.08.003.

Shand RD. 2003. Relationships between episodes of bar switching, cross-shore bar migration and outer bar degeneration at Wanganui, New Zealand. *Journal of Coastal Research* **19**(1): 157–170. ISSN 0749–0208.

Shand RD, Bailey DG. 1999. A review of net offshore bar migration with photographic illustrations from Wanganui, New Zealand. *Journal of Coastal Research* **15**(2): 365–378. ISSN 0749–0208.

Shand RD, Bailey DG, Shephard MJ. 1999. An inter-site comparison of net offshore bar migration characteristics and environmental conditions. *Journal of Coastal Research* **15**: 750–765.

Shand RD, Bailey DG, Shephard MJ. 2001. Longshore realignment of shore-parallel sand-bars at Wanganui, New Zealand. *Marine Geology* **179**: 147–161. doi: 10.1016/S0025-3227(01)00223-7.

Van Duin MJP, Wiersma NR, Walstra DJR, van Rijn LC, Stive MJF. 2004. Nourishing the shoreface: observations and hindcasting of the Egmond case, The Netherlands. *Coastal Engineering* **51**: 813–837. doi: 10.1016/j.coastaleng.2004.07.011.

Van Enckevort IMJ, Ruessink BG. 2003a. Video observations of nearshore bar behavior. Part 1: alongshore uniform variability. *Continental Shelf Research* **23**: 501–512. doi: 10.1016/S0278-4343(02)00234-0.

Van Enckevort IMJ, Ruessink BG. 2003b. Video observations of nearshore bar behaviour. Part 2: alongshore non-uniform variability. *Continental Shelf Research* **23**: 513–532. doi: 10.1016/S0278-4343(02)00235-2.

Van Rijn LC. 1993. *Principles of Sediment Transport in Rivers, Estuaries and Coastal Seas*. Aqua Publications: Amsterdam.

Van Rijn LC, Ribberink JS, van der Werf J, Walstra DJR. 2013. Coastal sediment dynamics: recent advances and future research needs. *Journal of Hydraulic Research* **51**(5): 475–493. doi: 10.1080/00221686.2013.849297.

Van Rijn LC, Walstra DJR, Grasmeijer B, Sutherland J, Pan S, Sierra JP. 2003. The predictability of cross-shore bed evolution of sandy beaches at the time scale of storms and seasons using process-based profile models. *Coastal Engineering* **47**(3): 295–327. doi: 10.1016/S0378-3839(02)00120-5.

Walstra DJR, Reniers AJHM, Ranasinghe R, Roelvink JA, Ruessink BG. 2012. On bar growth and decay during interannual net offshore migration. *Coastal Engineering* **60**: 190–200. doi: 10.1016/j.coastaleng.2011.10.002.

Walstra DJR, Hoekstra R, Tonnon PK, Ruessink BG. 2013. Input reduction for long-term morphodynamic simulations in wave-dominated coastal settings. *Coastal Engineering* **77**: 57–70. doi: 10.1016/j.coastaleng.2013.02.001.

Wijnberg KM, Terwindt JHJ. 1995. Extracting decadal morphological behavior from high-resolution, long-term bathymetric surveys along the Holland coast using eigen function analysis. *Marine Geology* **126**(1–4): 301–330. doi: 10.1016/0025-3227(95)00084-C.

Wijnberg KM, Wolf FCJ. 1994. Three-dimensional behaviour of a multiple bar system. *Proceedings of the Coastal Dynamics Conference*, Barcelona, Spain, 59–73.